Na$_2$TeO$_3$ represent examples of compacted and rigid crystalline networks.

Theoretically, $\langle u_0^2\rangle$ provides a measure of the first inverse moment (*14*) of the vibrational density of states of a network, that is,

$$\langle 1/\omega\rangle = 2M\langle u_0^2\rangle/3\hbar \qquad (8)$$

where M is the mass of the resonant atom and *h* is Planck's constant. The sensitivity of $\langle 1/\omega\rangle$ to floppy modes in a network glass was recently demonstrated. Both neutron (*16*) and ^{119}Sn Mössbauer (*14*) vibrational density of states measurements showed a systematic reduction of $\langle 1/\omega\rangle$ as $\langle r\rangle$ increased to 2.4, with the appearance of a discontinuity (change in slope) near the stiffness threshold in binary Ge-Se glasses. The observed discontinuity in $\langle u_0^2\rangle$ near $x_c = 0.18$ likewise constitutes evidence of a stiffness threshold in the tellurate glasses. This interpretation is independently confirmed by scanning calorimetry ($|dT_g/dx|$ and E_a) results (Fig. 2, A and B), which suggest that, near the privileged composition $x_c = 0.18$, these glasses are at a mechanically critical point, with a minimal configurational entropy change (*12, 13*) occurring upon melting of the glass at T_g.

In tellurate glasses, the observed stiffness threshold ($x_c = 0.18$) is close to the predicted value ($x_c = 0.20$) based on Eq. 7, but it is significantly different from the predicted value ($x_c = 0.25$) based on Eq. 2. These results underscore the importance of including broken β constraints due to NBO sites in describing the stiffness threshold in the tellurate glasses.

In earlier discussions (*14–17*) of the stiffness threshold in chalcogenides, it was tacitly assumed that β constraints about the chalcogens were intact. The directionality of covalent interactions stems from the hybridization of *s* and *p* orbitals. Replacement of S or Se by the more electronegative O anion in a network leads to an increased transfer of charge from the cation (Si, Na) to the anion and to a weakening of angular or β forces about the O anion as ionic interactions grow at the expense of covalent ones. The unusual GFT displayed by some of the oxides undoubtedly arises as a result of these broken β constraints, as revealed by the convergence of constraint theory predictions with the results of measurements of the ^{125}Te Lamb-Mössbauer factors presented here.

REFERENCES AND NOTES

1. H. Beyer, *Z. Kristallogr.* **124**, 228 (1967); O. Lindquist, *Acta Chem. Scand.* **22**, 977 (1968).
2. W. H. Zachariasen, *J. Am. Chem. Soc.* **54**, 3841 (1932); J. C. Phillips, *Solid State Phys.* **37**, 93 (1982).
3. A. K. Yakhind, *J. Am. Ceram. Soc.* **49**, 670 (1966); J. E. Stanworth, *J. Soc. Glass Technol.* **36**, 217 (1952); *ibid.* **38**, 183 (1954).
4. J. C. Phillips, *J. Non Cryst. Solids* **34**, 153 (1979); *ibid.* **43**, 37 (1981).
5. M. F. Thorpe, *ibid.* **57**, 355 (1983); H. He and M. F. Thorpe, *Phys. Rev. Lett.* **54**, 2107 (1985).
6. P. Boolchand and M. F. Thorpe, *Phys. Rev. B* **50**, 10366 (1994).
7. R. L. Mozzi and B. E. Warren, *J. Appl. Crystallogr.* **2**, 164 (1969); R. J. Bell and P. Dean, *Philos. Mag.* **25**, 1381 (1972); R. Zallen, *The Physics of Amorphous Solids* (Wiley, New York, 1983), pp. 72–73.
8. P. J. Bray and M. L. Lui, in *Structure and Bonding in Non Crystalline Solids*, G. E. Walrafen and A. G. Revesz, Eds. (Plenum, New York, 1983), pp. 285–289.
9. T. Sekiya, N. Mochida, A. Ohtsuka, M. Tonokawa, *J. Non. Cryst. Solids* **144**, 128 (1992); J. Heo, D. Lang, G. H. Sigel, E. A. Mendoza, D. A. Hensley, *J. Am. Ceram. Soc.* **75**, 277 (1992).
10. M. Zhang, G. Anaple, W. Bresser, P. Boolchand, D. McDaniel, unpublished material.
11. S. Neov, I. Gerassimova, K. Krezhov, B. Sybzhimov, V. Kozhakharov, *Phys. Status Solidi A* **47**, 743 (1978).
12. M. Zhang, W. Bresser, P. Boolchand, *J. Non Cryst. Solids* **151**, 149 (1992).
13. M. Tatsumisago, B. L. Halfpap, J. L. Green, S. M. Lindsay, C. A. Angell, *Phys. Rev. Lett.* **64**, 1549 (1990).
14. P. Boolchand *et al.*, *Solid State Ionics* **39**, 81 (1990).
15. W. Bresser *et al.*, *Phys. Rev. B* **47**, 11663 (1993).
16. W. A. Kamitakahara *et al.*, *ibid.* **44**, 94 (1991).
17. G. H. Dohler, R. Dandoloff, H. Bilz, *J. Non Cryst. Solids* **42**, 87 (1980).
18. We acknowledge discussions with B. Goodman and D. McDaniel. This work was supported by NSF grant DMR-92-07166.

14 June 1994; accepted 22 September 1994

Nickel Oxide Interstratified α-Zirconium Phosphate, a Composite Exhibiting Ferromagnetic Behavior

Boris Shpeizer, Damodara M. Poojary, Kyungsoo Ahn,
Charles E. Runyan Jr., Abraham Clearfield*

As part of an ongoing research program to synthesize novel pillared layered materials, nickel and cobalt hydroxyacetates were inserted between the layers of amine intercalates of α-zirconium phosphate. The structure of the resultant nickel composite, derived from x-ray powder data, was found to consist of a three-tiered layer of nickel atoms bridged by hydroxo and acetato groups. Heating to 420°C converted the hydroxyacetate layers to oxide and imparted ordered magnetic domains to the composite. The phosphate layers appear to act as a template directing the growth of the inserted layers in this class of composite materials.

Intercalation reactions of ions or molecules with layered solids are being used in novel ways to produce composites with useful properties such as ionic conduction, ion-exchange behavior, sorption, and catalysis (*1, 2*). The pillaring of clays may be viewed as an ion-exchange intercalative reaction. Smectite clay minerals swell in water, and in the colloidal state they may exchange their interlamellar ions for inorganic polymers such as $[Al_{13}O_4(OH)_{24}(H_2O)_{12}]^{7+}$. Because of the low layer charge of the clay and the high charge of the inserting polymer, the resultant composite is porous. These pillared clays are under study as a new class of acidic catalysts (*3–5*).

Many layered compounds other than clays are theoretically amenable to pillaring. However, they generally have a high ratio of charge to surface area and therefore do not swell spontaneously. In order to induce pillaring, Clearfield and Roberts (*6*) first intercalated an amine into α-zirconium phosphate, $Zr(HPO_4)_2 \cdot H_2O$, and into other phosphates. This reaction increases the spacing between the inorganic sheets by formation of an amine bilayer that could then be replaced by the pillaring species. This procedure has now become a common technique for pillaring (*7–10*). We report here on a similar reaction that has yielded interstratified materials containing sheets of NiO or CoO between zirconium phosphate layers; the resulting NiO composite is ferromagnetic.

To prepare the composite, we first intercalated crystalline α-zirconium phosphate with either hexylamine or octylamine. The resultant interlayer spacings were 22.9 and 28.7 Å, respectively. These intercalates were then mixed with solutions of $Ni(OOCCH_3)_2 \cdot 4H_2O$ or mixtures of nickel nitrate and nickel acetate and refluxed for different lengths of time. The final products had interlayer spacings of 18.4 to 19.5 Å. A typical preparation involved dissolving 8.39 g of hexylamine (82.9 mmol) in 200 ml of water and then adding 10 g of solid crystalline α-zirconium phosphate (33.1 mmol). The mixture was stirred for 24 hours at room temperature. The solid phase was filtered off and washed extensively with doubly distilled water and a final wash with 50 ml of

---

Department of Chemistry, Texas A&M University, College Station, TX 77843, USA.

*To whom correspondence should be addressed.

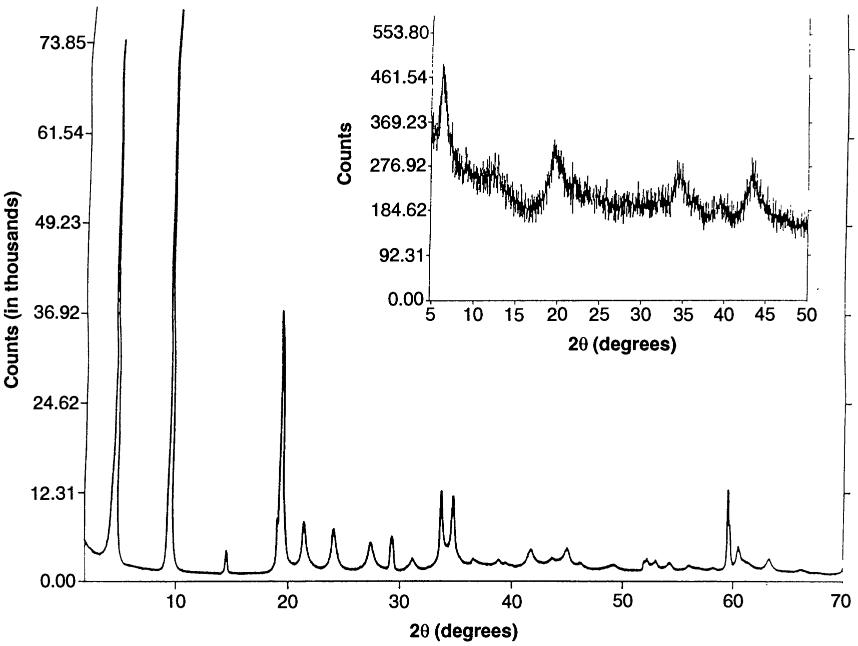

Fig. 1. X-ray powder diffraction pattern of α-zirconium phosphate after refluxing with $Ni(OOCCH_3)_2 \cdot 4H_2O$ for 24 hours. (Inset) The powder pattern after heating to 400°C. Bragg angle, 2θ.

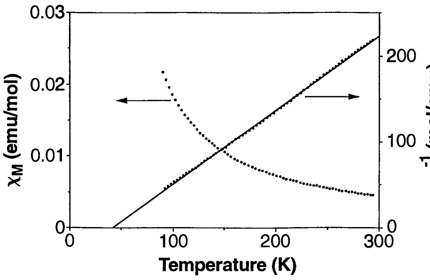

Fig. 3. Magnetic susceptibility per mole (χ_M) of Ni atoms of $Zr(PO_4)_2Ni_4(OH)_5(C_2H_3O_2) \cdot 2H_2O$. The plot of the inverse of the molar susceptibility is fit with a straight line.

acetone. The sample was dried at 65°C to yield 15.44 g of the amine intercalate (yield, 95.8%), $Zr(HPO_4)_2(C_6H_{13}NH_2)_2$. We prepared a solution by dissolving 18 g (61.9 mmol) of $Ni(NO_3)_2 \cdot 6H_2O$ and 18 g (72.3 mmol) of $Ni(O_2CCH_3)_2 \cdot 4H_2O$ in 200 ml of doubly distilled water. To this solution was added 2 g (4.12 mmol) of the zirconium phosphate hexylamine intercalate, and the mixture was refluxed for 24 hours. The solid was recovered from the solution by centrifugation, washed extensively with doubly distilled water, and dried in a desiccator. Elemental analysis gave the following composition: Zr, 13.65%; P, 8.66%; Ni, 35.96%; and C, 3.02%; the calculated analysis for $Zr(PO_4)_2Ni_4(OH)_5(C_2H_3O_2) \cdot 2H_2O$ is as follows: Zr, 13.23%; P, 8.89%; Ni, 33.69%; and C, 3.44%. The yield of product was 2.73 g or 95.1% based on the above formula. Weight loss curves determined by thermogravimetric analysis indicate a loss of 1 mol of water to 130°C and the loss of a second mole from 130° to 300°C. This weight loss was followed by a sharp loss of ~12% between 400° and 500°C. The total weight loss averaged 19.0%; the weight loss calculated for the above composition converting to $ZrNi_4O_3(PO_4)_2$ at elevated temperature is 18.9%, in excellent agreement with the observed value. The cobalt analog was prepared in a similar fashion.

All of the preparations yielded more detailed x-ray powder patterns than any known pillared layered material. The x-ray diffractogram for the most highly crystalline sample, before heating to remove water and acetate groups, is shown in Fig. 1. Unit cell dimensions were extracted from this x-ray pattern and refined by least squares methods (*11*) to yield $a = 9.298(2)$ Å, $b = 5.389(1)$ Å, $c = 37.616(5)$ Å, $\beta = 103.40(2)°$, and number of formula units per cell $Z = 4$ (numbers in parenthesis indicate errors in the last digit). Systematic absences $hk\ell$, $h + k = 2n + 1$ and $h0\ell$, $\ell = 2n + 1$ indicated that the space group is either Cc or $C2/c$. The symmetry and cell dimensions indicate that the zirconium phosphate layer is intact in the crystal lattice (*11*, *12*).

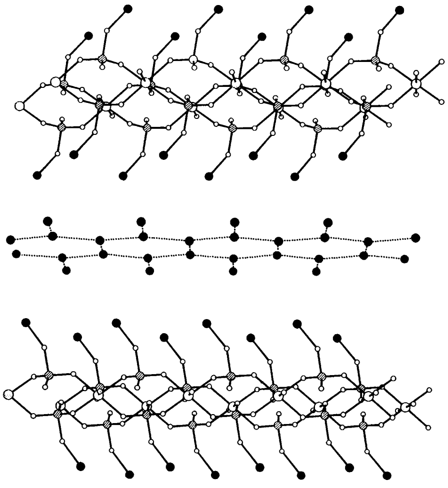

Fig. 2. Schematic representation of the arrangement of Ni atoms between the layers of α-zirconium phosphate. The connectivity between Ni atoms is through hydroxyl, acetate, or water oxygens. Zr (lightly shaded circles), P (hatched symbols), O (small, open symbols), and Ni (solid symbols). Hydroxyl and acetate groups bonding Ni atoms together are omitted.

A model for the layer was then built on the basis of the cell dimensions and refined against the powder pattern. The refinement was carried out isotropically (*13*) in the centrosymmetric space group with soft constraints for bond distances and angles in conformity with known values for zirconium phosphate layers (*12*). A difference map computed at this stage revealed the positions of the Ni atoms. They take the form of a three-tiered layer, as shown in Fig. 2. Oxygen atoms in the interlayer region have been omitted for clarity but also because all of their positional parameters have not yet been determined. However, ultraviolet-visible spectra show that the Ni atoms are octahedrally coordinated. Absorption maxima were found at 380 and 660 nm. The Ni atoms in the middle tier are arranged in the form of a hexagonal sheet. In this sheet each Ni atom is linked to three neighboring Ni atoms by hydroxo, aquo, or acetato bridges. The remaining Ni atoms are located between the central NiO sheet and the phosphate layers and are bonded to the host layers through the P–O$^-$ groups. This connectivity must have occurred through a condensation reaction, either with an Ni(OH) group to split out water or an acetate group to form acetic acid. These Ni

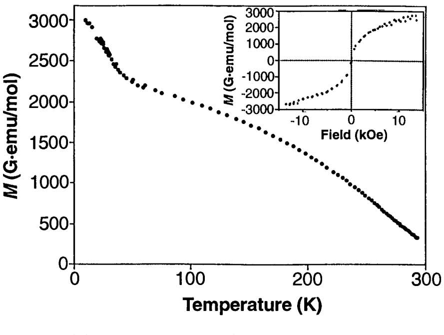

Fig. 4. Molar magnetization versus temperature for each mole of Ni atoms of $Zr(PO_4)_2Ni_4O_3$ at 8 kG from 10 to 295 K. (Inset shows the field dependence at 77 K.) The scatter in data points below 70 K reflects the fact that these data were obtained in both the cooling and warming directions.

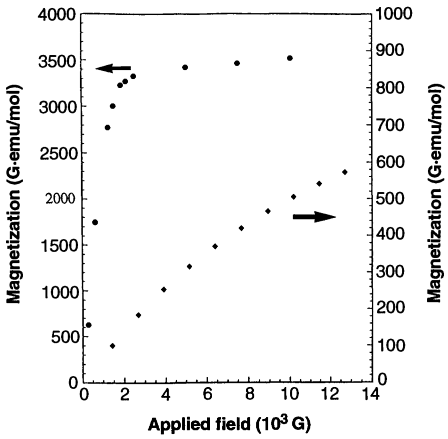

Fig. 5. Comparison of magnetization versus applied field for Ni metal (●) (left scale) and for Ni-pillared α-ZrP (◆) (right scale) after calcination.

atoms are about 5 Å from the Ni central layer, and thus they are not directly connected to the central layer.

Magnetic susceptibility measurements were carried out on several samples of $Zr(PO_4)_2$-$Ni_4(OH)_5(C_2H_3O_2)\cdot 2H_2O$ and $Zr(PO_4)_2Ni_4O_3$ by the Faraday method at a field of 8 kG over a temperature range of 10 to 300 K. Quantitative samples (20 to 40 mg) were contained in carefully dried capsules (Kel-F), the susceptibilities of which were measured in separate runs and corrected for core diamagnetism and container contributions. The composite that formed at room temperature is paramagnetic, as shown by the data in Fig. 3. The magnetic moment μ_{eff} per Ni is 2.997 Bohr magnetons, which is slightly higher than the spin-only moment (2.83 Bohr magnetons) but well within the range observed for d^8 Ni atoms. On heating to 400°C, the magnetic behavior of the composite changes as shown in Fig. 4. The observed behavior is neither that of a paramagnetic substance nor that of a bulk ferromagnet. However, it does exhibit features that may be attributed to magnetically ordered particles or to ordered domains within particles. In fact, the particles are strongly drawn to a magnet as if they were ferromagnetic. The magnetization of the heated composite increased with applied field up to 15,000 G but did not reach saturation (Fig. 5) (*14*).

The x-ray powder pattern of a sample heated to 400°C is shown in the inset to Fig. 1. The interlayer spacing of the heated sample is 14.6 Å. The elimination of acetate ion and water molecules and the splitting out of water from the hydroxyl groups are responsible for the reduction in the interlayer spacing. In the process the Ni ions bonded to phosphate groups must move to within 3.5 Å of the central layer and bond to it through oxygen, creating three-tiered NiO-like layers sandwiched between the zirconium phosphate layers. Because the thickness of the zirconium phosphate layer is 6.3 Å, the NiO layer is then 8.3 Å thick, a reasonable value for a three-tiered Ni–O layer. During heating the sample turns gray to black, but, on standing, its original green color returns. Exposure to light as in the ultraviolet-visible spectrometer restores the black color. This feature prevented us from obtaining an electronic spectrum of the heated composite.

Interestingly, the heated composites are microporous with surface areas of 60 to 130 m^2/g. The pores are relatively uniform with average diameters of ~10 Å. The pores may arise from defects that cause the growth of the NiO layers to terminate and these layers to exist as islands with gaps between these NiO islands. The fact that the nickel hydroxide layers are bonded to the phosphate groups of the zirconium phosphate layers before heating to elevated temperatures leads us to believe that the phosphate layers act as a template to direct the growth of the metal hydroxo layers (*15*).

REFERENCES AND NOTES

1. M. S. Whittingham and A. J. Jacobson, Eds., *Intercalation Chemistry* (Academic Press, New York, 1982).
2. T. E. Mallouk and H. Lee, *J. Chem. Educ.* **67**, 829 (1990).
3. T. J. Pinnavaia, *Science* **220**, 365 (1983).
4. A. Clearfield, in *Surface Organometallic Chemistry: Molecular Approaches to Surface Catalysis*, J. M. Basset, Ed. (Kluwer Academic, Dordrecht, Netherlands, 1988), p. 271.
5. R. Burch, Ed., special issue, *Catal. Today* **2**, 185–366 (1988).
6. A. Clearfield and B. D. Roberts, *Inorg. Chem.* **27**, 3237 (1988).
7. S. Cheng and T. C. Wang, *ibid.* **28**, 1283 (1989).
8. S. Hardin, D. Hay, M. Mullikan, J. W. Sanders, T. W. Turney, *Chem. Mater.* **3**, 997 (1991).
9. M. E. Landis *et al.*, *J. Am. Chem. Soc.* **113**, 3989 (1991).
10. K. Wade, thesis, Texas A&M University (1993).
11. D. M. Poojary, H.-L. Hu, F. L. Campbell III, A. Clearfield, *Acta Crystallogr. Sect. B* **49**, 996 (1993).
12. A. Clearfield and G. D. Smith, *Inorg. Chem.* **8**, 431 (1969); J. M. Troup and A. Clearfield, *ibid.* **16**, 3311 (1977).
13. Structure refinement by the whole-pattern Rietveld method was effected with GSAS: A. Larsen and R. B. Von Dreele, Generalized Structure Analysis System (Los Alamos Neutron Scattering Center, Los Alamos National Laboratory, Los Alamos, NM, copyright 1985–1988 by the Regents of the University of California).
14. Detailed measurements of both the Ni and the Co composites heat-treated in the range 400° to 700°C are in progress.
15. We are testing this hypothesis by carrying out similar reactions with other layered compounds and examining the structures of the interposed layers.
16. This study was supported by NSF grants DMR-9107715 and INT-9015164. We thank T. Hughbanks for helpful discussions on the magnetic behavior of the composites.

9 May 1994; accepted 22 September 1994

The Validity of the "Diradical" Hypothesis: Direct Femtosecond Studies of the Transition-State Structures

S. Pedersen, J. L. Herek, A. H. Zewail*

Direct studies of diradicals, the molecular species hypothesized to be archetypal of chemical bond transformations in many classes of reactions, have been made using femtosecond laser techniques with mass spectrometry in a molecular beam. These studies are aimed at "freezing" the diradicals in time and in the course of the reaction. The passage of these species through the transition-state region was observed and the effect of total energy and alkyl substitution on the rates of bond closure and cleavage was examined. The results establish the nature of these intermediates and define their existence during reactions.

For the past 60 years, the concept of diradicals as intermediates has been hypothesized to be archetypal of chemical bond transformations in many classes of thermally activated as well as photochemical reactions. Since the development of extended Hückel theory, Woodward-Hoffmann rules, and frontier-orbital descriptions of bonding (*1*), diradicals have become central to the understanding of reaction mechanisms as well as to the predictability of reaction products, rates, and stereochemistry. One of the most well-studied reactions, both theoretically and experimentally, is the ring opening of cyclobutane to yield ethylene or the reverse addition of two ethylene molecules to form cyclobutane:

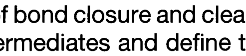

Scheme 1.

Such a reaction is a classic case study for a Woodward-Hoffmann description of concerted reactions. The reaction may pro-

---

Arthur Amos Noyes Laboratory of Chemical Physics, California Institute of Technology, Pasadena, CA 91125, USA.

*To whom correspondence should be addressed.